Materials Science Forum Vol. 590 (2008) pp 141-174
online at http://www.scientific.net

Present status of deep UV nitride light emitters

Asif Khan and Krishnan Balakrishnan

Department of Electrical Engineering, University of South Carolina, 301 S. Main Street, Columbia, South Carolina 29208, U.S.A.
asif@engr.sc.edu

Keywords: MOCVD, AlN, GaN, AlGaN AlInGaN, UV, deep-UV, light-emitting diode, laser diode, epitaxy, growth, pulsed lateral overgrowth.

Abstract. Ultraviolet light emitting diodes with emission wavelengths less than 400 nm have been developed using the AlInGaN material system. Rapid progress in material growth, device fabrication and packaging enabled demonstration of deep-UV light-emitting devices with emission from 400 to 210 nm with varying efficiencies. For high aluminum alloy compositions needed for the shorter wavelength devices, these materials border between having material properties like conventional semiconductors and insulators, adding a degree of complexity to developing efficient light emitting devices. This chapter provides a review of III-nitride based UV light emitting devices including technical developments that allow for emission in the ultraviolet spectrum, and an overview of their applications in optoelectronic systems.

Introduction

Applications using III-Nitride emitters including indicator lights, commercial signage, automotive lighting, and high density optical storage have been increasing rapidly leading to an expansion of the markets for light emitting diodes (LEDs) and laser diodes (LDs). Recently, the feasibility of using solid-state lighting for general illumination has been established with development of LEDs emitting greater than 100 lumens of optical power (comparable to a 60W light bulb), with efficiency in excess of ~100 lm/W depending on the color temperature [1]. The market size for these high brightness LEDs is well over $4 Billion/yr with the relatively new laser diodes' market in excess of $35 Million/Yr despite stringent patent restrictions on the products [2,3]. The impact making development of III-nitride semiconductors has been taking place only in the last two decades, much later than other conventional semiconductors such as silicon and GaAs. Lack of suitably lattice matched substrates and the difficulty of incorporating nitrogen into the III-nitride semiconductors were the main causes for the delay in their development. In the late 1980s and early 1990s, experimental procedures were developed that enabled the growth of high quality single crystal materials of binary and ternary III-nitride semiconductors, such as GaN, InGaN and AlGaN, by using low temperature nucleation layers of either AlN or GaN [4,5]. This was followed by the realization p-type GaN using Low Energy Electron Beam Irradiation (LEEBI) and subsequently by thermal annealing [6,7]. These major breakthroughs paved way for the development of commercial III-nitride based visible and long wavelength UV optical devices. With the "visible" light emission device technology reaching its maturity, the major focus has been shifted towards the shorter wavelength ultraviolet devices. This interest is ignited by the potential applications for the UV LEDs in air- and water purification, germicidal and biomedical instrumentation systems, and for the UV LDs in medical surgery and other uses [8]. The quantum efficiency of the near ultraviolet (UV) LED received a huge boost with advanced growth, metallization and packaging techniques. The emission wavelengths of LEDs now cover the majority of the UV spectrum ranging from 400 nm to 210 nm [9]. UV laser diode emission has shifted towards shorter wavelengths with viable operation demonstrated in the range 340 nm – 350 nm.

The UV portion of the electromagnetic spectrum lies in the wavelength range 10 nm – 400 nm. The UV spectrum is classified in to four distinct regions: UV-A or long-wave UV (320 nm – 400 nm), UV-B or mid-wave UV (290 nm – 320 nm), UV-C or short-wave UV (200 nm – 290 nm) and vacuum UV (10 nm – 200 nm). III-nitride based LEDs have the theoretical capability to emit at all wavelengths in the UV-A, B and C, with 210 nm – 400 nm LEDs already demonstrated. The emission wavelength is dictated by the fundamental band gap of the material used in the active region of the device, with AlN having a bandgap corresponding to an emission wavelength of approximately 200 nm, GaN to a wavelength of 365 nm, and low indium composition InGaN having a band gap corresponding to an emission wavelength of approximately 400 nm. The deep ultraviolet (DUV) refers to UV-B and UV-C wavelength regions.

DUV emitters offer a variety of options primarily due to the interaction between UV radiation in this wavelength regime and biological species. High density optical storage, efficient white LEDs, water and food sterilization, portable biological and chemical agent detection systems, non-line of sight communication (NLOS) and others. It must be also mentioned that the absorption of radiation by the atmospheric ozone is very strong for UV wavelengths shorter than ~280 nm, resulting in very little solar radiation in this wavelength regime being present near the earth's surface. Hence, biological organisms on earth have never developed a tolerance for this radiation. Therefore, the man-made UV-C light source has become a vital tool in the treatment and destruction of bacterial, yeast, viruses and fungi. Mercury, Xenon and Deuterium lamps with emission spectrum ranging from 254 nm to about 290 nm have been used extensively for purification of microbiological contaminants in air and water. However, their high operating voltages and larger size together with the environmental hazards of using mercury, preclude their use in techniques for disinfection, for air and water purification and in biomedicine. Added to that, these sources have relatively shorter life time when compared with III-nitride based UV emitters, lack of wavelength choices or tunability, power modulation difficulty, environmental pollution and a few other negatives make them worthless to persist with. Replacement of these conventional sources with III-N semiconductor detectors will solve most of these problems and offer several additional advantages including miniaturization, reliability, reduced costs, low power consumption, and ultimately a choice of wavelength of operation between 365 nm and 200 nm. Figure 1 presents some applications requiring UV radiation: a) industrial spot curing b) treatment of psoriasis by UV phototherapy and c) air and water purification.

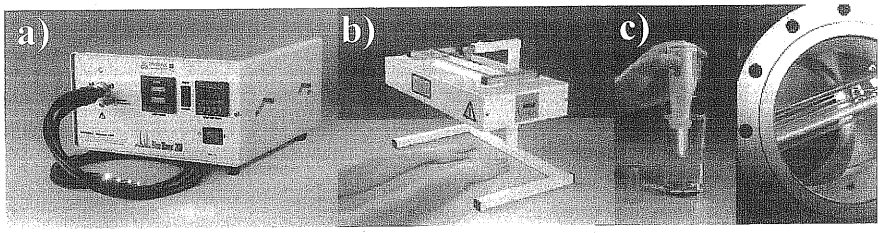

Figure 1: Applications requiring DUV radiation: a) industrial spot curing b) treatment of psoriasis by UV phototheraphy by a 308 nm lamp, and c) air and water purification.

In this chapter, the progress and the current status of the III-nitride DUV emitters are discussed. As the development of many aspects of DUV emitters is connected with their long wavelength counterparts, nitrides based UV emitters in the UV-A are also discussed. The UV LEDs are discussed under two broad sections namely long wavelength UV LEDs (covering UV-A LEDs) and DUV LEDs (covering both UV-B and UV-C LEDs). Since device operation in the DUV region requires primarily AlGaN based active layers with very high Al molar fraction in the alloy some

pertinent material issues and challenges in the material growth are discussed. The problems of strain, cracking and defects in AlGaN layers heteroepitaxially grown over sapphire substrates are included. Problems of doping of AlGaN are also covered along with the discussion of the AlGaN bandgap bowing.

Long wavelength UV LEDs

The technology for the long wavelength or UV-A light emitters with emission at wavelengths longer than 365 nm is fairly well established as it was developed simultaneously with the visible blue-green light emitters. Due to the similarity in recombination mechanisms and device design with visible light emitters, the UV-A devices were relatively easier to manufacture when compared with the deep-UV devices. The 365 nm – 400 nm emission LEDs are now widely available, with most of the commercially available devices utilizing InGaN quantum wells. UV-A devices on GaN substrates exhibit increased efficiency compared with the devices grown on sapphire. This is a result of the reduction in the threading dislocation density (TDD) as a result of using the low dislocation density native bulk or quasi bulk substrate material. In addition to the TDDs, as the emission wavelength approaches 365 nm, GaN and particularly p-type GaN becomes absorbing which can greatly affect the extraction of light from the semiconductor chip. Morita et al have developed 365 nm LEDs with a "GaN-Free" device structure that is achieved through laser assisted liftoff/separation of the GaN from the sapphire substrate, followed by removal the of the exposed GaN [10]. This resulted in 365 nm LEDs with EQE's in excess of 5%, despite being grown initially using a conventional MOCVD GaN on sapphire growth approach. Subsequently, it has been demonstrated that utilizing the same approach (substrate and GaN removal) but on GaN substrates resulted in increased efficiency and device lifetime compared to devices grown on several microns of GaN on sapphire due to the lower TDD from the starting bulk GaN material [11]. These devices are now commercially available and large power chips (~ 1 mm x 1 mm) offer 250 mW of CW output power at 365 nm with an injection current of 500 mA, corresponding to an external quantum efficiency (EQE) of 14.7%. Smaller conventional size LED chips are available in wavelengths ranging from 365 – 395 nm with typical output powers at 20 mA ranging from 2–10 mW.

The UV-A LEDs with emission wavelengths less than 365 nm require AlGaN active regions and these to date have not achieved the same efficiency as the GaN/InGaN LEDs. Various methods were adopted to achieve LEDs with emission wavelengths below 365 nm (the band edge of GaN). The first GaN-AlGaN multiple quantum well with emission at 330-365 nm was demonstrated by Khan et al.[12]. The UV-A emission was achieved by changing the transition energy through quantum confinement in the GaN quantum wells. This is similar to the approach used to fabricate 365 nm LEDs with $In_{0.01}Ga_{0.99}N$ QW's. Subsequently, Han et al.[13] used an $Al_{0.2}Ga_{0.8}N$/GaN multiple quantum well (MQW) structure to achieve the emission at 353 nm. An output power of 13 μW at 20 mA was achieved, and the corresponding external quantum efficiency was much less than 1 %. To shift the emission wavelength below 350 nm, several groups employed $Al_xGa_{1-x}N/Al_yGa_{1-y}N$ MQWs [14,15] or a double heterostructure (DH) active layer [16]. Another approach used to achieve shorter wavelength emission was the utilization of quaternary AlInGaN employed by Khan et.al. [17]. Because the presence of In in the active regions of visible LEDs leads to greatly improved efficiencies, attempts have been made to include small amounts of In in UV LEDs as well. Subsequently 340 and shorter wavelength UV A LEDs were achieved by using the AlInGaN quaternary epilayers. Several other groups had demonstrated that the introduction of In into ternary AlGaN alloys could improve the optical quality of the AlGaN layers and thus the optical and electrical properties of the LEDs [18,19,20,21,22]. The quaternary AlInGaN MQW active region was grown using pulsed atomic layer epitaxy (PALE) which has been shown to result in better quality of the material in the quaternary layers because the PALE method gives better control of the composition and surface morphology [23,24]. Kinoshita et al.[25] reported an LED on SiC with emission at 333 nm by incorporating a Mg-doped $Al_{0.25}Ga_{0.75}N$/GaN superlattice (SL) similar to that of Nishida et al [26]. The superlattice was claimed to improve the hole injection into

the active region. For all these developments on UV-A LEDs, the emission intensity was considerably lower than that of the III-nitride visible LEDs with InGaN-GaN quantum wells in the active region.

Causes for poor efficiency of UV light emitters. The low efficiency of the UV light emitters, especially deep-UV devices, is believed to be caused by some prominent factors, namely, Quantum Confined Stark Effect (QCSE), Poor Alloy Clustering, Low Carrier Confinement and Absorbing p-GaN contact layers.

The QCSE is caused by the strong spontaneous and piezoelectric fields in the quantum wells composed of III-nitride materials [27,28]. For the III-N materials, these fields get stronger with increasing aluminum alloy compositions that are needed for the UV emission devices. These electric fields lead to reduced radiative recombination efficiency. The QCSE bends the semiconductor valence and conduction bands leading to a physical separation of the electron and hole pairs. This reduces their recombination probability in the quantum wells which in turn leads to reduced emission efficiencies [29].

Poor alloy clustering was believed to be the reason for the unusually high emission efficiency for visible emitters, given the relatively large TDD ($>10^8$ cm^2) in the active region. Formation of indium rich clusters physically confined the carriers in the InGaN-GaN quantum wells and separated them from the threading dislocations (TDs). Absence of this alloy clustering in GaN and AlGaN quantum wells of the UV emission devices is believed to reduce their radiative recombination efficiency. However, the hypothesis of In-clustering is disputed more recently by Smeeton *et al* through their TEM analysis results [30]. The TEM measurements performed on samples under various incident electron beam dosages showed a correlation between their measurement conditions and the observed "alloy clustering". Based on this new finding, continued exploration of recombination physics for both InGaN/GaN QW's, and their AlGaN/AlGaN UV counterparts is necessary to determine whether there are any fundamental differences in the active regions of visible and UV LEDs and their respective recombination mechanisms.

Low Carrier Confinement in the active region of the UV and DUV light emitters is one of the major causes why their efficiencies are considerably inferior when compared with their visible counterparts. Early reports of UV LEDs commonly showed multiple emission peaks at long wavelengths, indicating loss of carriers to regions other than the active region and hence unintended radiative transitions. At the time, it was unclear whether this resulted from deep level transitions in the quantum wells, or from recombination occurring outside of the active region. It was, however, observed that the addition of p-type AlGaN above the QW's reduced the intensity of the deep level peaks, indicating that the deep level resulted from electrons passing through the active region and recombining with holes in the p-type material [31]. Confinement of the electrons using a higher aluminum composition AlGaN electron blocking layer between the QW's and p-type contact layer was determined to be more critical than efforts to confine holes using a similar hole blocking layer between the QW's and the n-AlGaN contact layer, due to the low mobility and injection efficiency of the holes compared to electrons. Similar electron blocking layers are commonly used for blue InGaN/GaN LEDs and laser diodes to avoid long wavelength emission.

Absorbing p-GaN contact layers used in the UV emitters with emission wavelengths less than 365 nm considerably reduces their efficiency. This problem is more severe for the DUV devices. In addition, UV emission from the active region is absorbed by the thin metal contacts used in the devices. UV absorbing substrates, such as GaN, SiC, etc., when used, also cause absorption problems for the devices. Although substrate absorption limited the extraction efficiency of the early devices, several groups were able to demonstrate that defects in the material also greatly decrease the efficiency of these devices and obtain reasonable output powers even for devices grown on absorbing substrates. A 352 nm LED with EQE of 1% was measured for a device grown on a free-standing GaN substrate, with typical dislocation density of ~1 x 10^6 cm^{-2} [32]. Edmond et al. also demonstrated 340 nm LEDs with an EQE of 4% grown on absorbing SiC by implementing a Broad Area Defect Reduction (BADR) growth technique by which silicon nitride defect masks are deposited on the surface in a random orientation to block crystalline defects from propagating into

the active region of the LED [33]. This work demonstrated the potential for much higher power UV emitters due to current limitations both with internal and extraction efficiency of the devices. Despite the still relatively low quantum efficiency, compared with visible LEDs, UV-A LEDs are starting to find applications in fluorescence spectroscopy, and industrial curing [34,35].

DUV Light Emitting Devices

As described in the initial part of this chapter, there are strong reasons for desiring the development of solid-state devices emitting in the DUV region. The key events related to the development of DUV light emitting devices are presented in Table 1.

Major developments	Research group, Year
Low temperature AlN buffer layer	Amano et al., 1989 [4]
AlGaN-GaN-AlGaN MQW	Khan et al., 1990 [11]
p-type GaN by Low Energy Electron Beam Irradiation (LEEBI)	Amano et al, 1990 [6]
Low temperature GaN buffer layer	Nakamura et al., 1991 [5]
AlGaN/GaN MQW LED	Han et al., 1998 [12]
Smooth AlN with low V/III ratio	Ohba et al., 1996 [36], 2001 [37]
352 nm LED on bulk GaN	Nishida et al., 2001 [26]
340 nm UV LED	Adivarahan et al., 2001 [38]
315 nm LED	Khan et al., 2001 [39]
305 nm UV-LED	Khan et al., 2001 [39]
AlN/AlGaN SL for thick & crack-free n-AlGaN	Zhang et al., 2002 [40]
UV-LED 285 nm	Adivarahan et al., 2002 [41]
GaN free UV LED (365 nm)	Morita et al., 2002 [9]
280 nm LED	Yasan et al., 2002 [102]
365 nm - Laser Diode (cw)	Masui et al., 2003 [152]
359.7-361.6 – Laser Diode (pulsed)	Kneissl et al., 2003 [140]
354.7 nm – Laser Diode (pulsed)	Masui et al., 2003 [152]
350.9 nm – Lased Diode (cw)	Iida et al., 2004 [155, 156]
348 nm - Laser Diode (cw)	Edmond et al., 2004 [33]
343 nm – Laser Diode (pulsed)	Edmond et al., 2004 [33]
269 nm LED	Adivarahan et al., 2004 [90]
254 nm LED	Wu et al., 2004 [117]
250 nm LED	Adivarahan et al., 2004 [115]
210 nm AlN LED	Taniyasu et al., 2006 [124]
Stimulated emission from AlN at 214 nm	Shatalov et al., 2006 [42]
High temperature AlN growth (1500°C)	Balakrishnan et al. 2006 [69]
MOHVPE AlN growth	Fareed et al. 2006 [43]

Table 1: Summary of the major developments that took place during the development of III-nitride based UV emitters.

The primary difference between UV-B/C devices and the previously discussed UV-A devices is that it was no longer possible to use a GaN base layer, as was commonly used for the UV-A devices, due to the much larger tensile strain that results for AlGaN grown on GaN. This leads to cracking of the AlGaN films and catastrophic failure for LED devices. Increasing the aluminum composition (needed for the DUV devices) also leads to difficulties in the growth of high structural

quality material, typically resulting in an even higher dislocation density for AlGaN alloys compared to GaN. It also leads to difficulties in doping the material to impart it n-type and p-type conductivity.

Growth of $Al_xGa_{1-x}N$. In order to fabricate deep-UV light emitters, low defect density AlN and AlGaN materials are needed. The growth of $Al_xGa_{1-x}N$ has proved to be significantly more difficult when compared with that of GaN. This problem is partially due to the fact that Al-adatoms have a much larger sticking coefficient than Ga-adatoms. It is well known that layer-by-layer growth of films with attachment of ad-atoms at steps or kinks gives the smoothest surface features, as opposed to three dimensional island growth. Because Al-adatoms have a low mobility on the surface, they are less likely to be able to move from their point of impact from the vapor, and rather than incorporating at the most energetically favorable lattice sites such as at a step, they tend to cause islands to nucleate which disturb the epitaxial growth. As a result, higher densities of extended defects such as dislocations and grain boundaries are much easier to generate as these growth islands from different nucleation sites coalesce. Moreover, in the MOCVD growth of $Al_xGa_{1-x}N$ layers, the commonly used Al-metalorganic precursors (trimethylaluminum, TMA and triethylaluminum, TEA) are known to be more reactive than their Ga-based counterparts. Hence gas-phase reactions and related adduct formations tend to interfere with the growth process. Figure 2 presents an experimental plot for Al-incorporation in the solid film as a function of the Al-fraction in the gas phase [44]. Under such growth conditions, the Al-incorporation is very efficient when the gas phase fraction is smaller than 50% (molar fraction: TMA/(TMA+TMG)). Above 50%, a reduced level of incorporation has been observed due to the gas-phase reaction between TMA and NH_3. This reaction could interrupt the normal epitaxial growth process by generating nano- or micro-particles which fall onto the growing surfaces. As a result, for high-Al-content AlGaN, to avoid surface roughening, pits and particles, and associated structural defects, a lower growth rate must be employed. Other critical problems affecting epitaxial growth of high quality AlGaN films include film cracking and poor electrical conductivity. These factors present great challenges for device development efforts, and require a full exploration of the materials deposition domain for AlGaN, including the introduction of extensive innovative approaches. Some of the major approaches attempted to resolve these problems are now presented.

Recently, there have been major developments in the production of native substrates including GaN, AlN, and their alloys as free-standing wafers using a variety of growth techniques [45-48]. However, the stage has not been reached where these substrates of consistently high quality and size required for commercial device production are available. Due to this reason, nitride thin films tend to be grown on foreign substrates, a process known as hetero-epitaxy. Commonly used substrates include sapphire (Al_2O_3), SiC, Si, and GaAs. For each foreign substrate there are differences in the lattice parameters and the thermal expansion coefficients compared with the nitride materials. In addition to the formation of threading dislocations, the nitride films tend to be bowed and even cracked. The usefulness of low temperature buffer layers for improving the quality of hetero-epitaxial GaN films has been recognized since 1986 [4]. Because the problems with AlGaN films are even more severe, researchers have developed novel approaches based on the idea of compliant-layer-insertion. Kamiyama et al.[49] and Han et al.[50] individually adapted low-temperature (LT) AlN and AlGaN insertions to avoid cracking of AlGaN grown on GaN. The periodic insertion of LT-grown AlGaN layers was shown to effectively reduce the biaxial tensile strain in the AlGaN films, thus reducing the cracking [50]. The LT-grown films tend to exhibit poorer structural quality and hence to possess less stiffness. The LT films are more elastic, making them more compliant and able to accommodate more strain. However, this method could still introduce dislocations after each LT-layer insertion. Besides, there are too many thermal cyclings during one growth which also makes the technique less attractive.

Epilayer Al-fraction

Figure 2: A
p
A
s
o
g

An
order of
substrates.
because fr
experience
for this kir
often obse
islands wh
blocks) be
through at
boundaries
area, and t
energy fro
released ei
system wh
sapphire c
generate ir
avoided by
mosaic blo
(PALE) ap
approach,

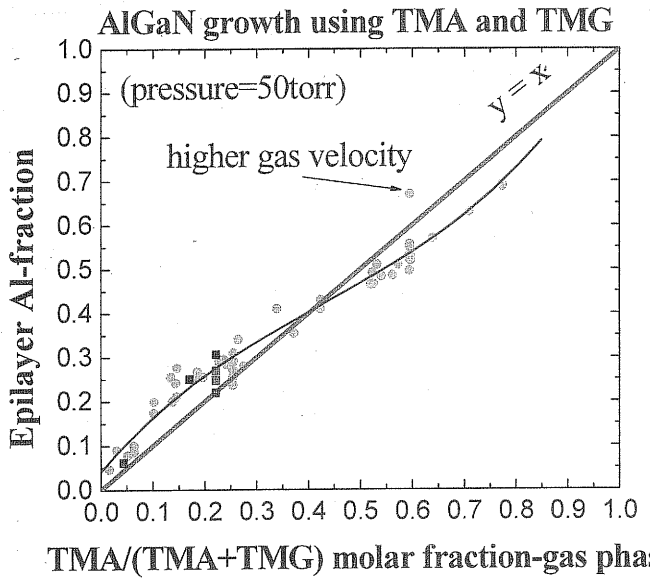

Figure 2: Al-composition in the AlGaN layers as a function of Al-fraction in the gas phase. Under the used growth conditions, Al-incorporation is efficient when the Al- gas-fraction is less than 50%. Above 50%, a reduced Al-composition in solids compared to gas phase indicates a pronounced gas-phase reaction has occurred. High gas velocity (including lower growth pressure and high push gas) could increase Al-incorporation.

An alloy composition with a low V/III ratio (about 1:4) and high growth temperatures in the order of 1200°C were used to achieve a two-dimensional growth mode for AlN on sapphire substrates. The cracking of AlGaN films grown on basal plane sapphire substrates is surprising because from the lattice and thermal mismatch point of view, AlGaN grown on sapphire should experience biaxial compressive strain, which could not cause cracking at all. The strain responsible for this kind of cracking is rooted in a different mechanism and is called intrinsic tensile strain, often observed in imperfect materials (polycrystalline) growth. It arises from the coalescence of islands where the film consists of discrete mosaic blocks. During growth when two islands (mosaic blocks) begin to approach each other at a certain distance, these islands will begin to coalesce through atomic rearrangement to allow a minimized system free energy by reducing two surface boundaries to one. This process however will generate tensile strain in the vicinity of the zipped area, and the strain is inversely proportional to the square root of the island dimension [51]. The energy from the tensile strain will therefore build up with film thickness, to a point where it will be released either by dislocation generation or by cracking. Cracking is likely to happen in a material system where dislocations have no slip system, like in AlGaN films. AlGaN films grown on sapphire consist of many fine mosaic blocks and the coalescence of these mosaic blocks will generate intrinsic tensile strain, so eventually the film must crack. This kind of cracking can be avoided by improving the material quality, i.e., by decreasing the material mosaicity (increasing the mosaic block dimensions). It has been suggested by Khan et al. that the pulsed atomic layer epitaxy (PALE) approach could be used to grow high quality AlN and AlGaN films [52-54]. In the PALE approach, the flow rates of group III and group V precursors are sequentially modulated enhancing

surface migration of Al- and Ga-adatoms, which resulted in better crystalline quality and surface morphology of epitaxial layers. Another approach was suggested by Bykhovsky et al. who theoretically predicted elastic strain relaxation in GaN/AlN and GaN/AlGaN superlattices [55]. Zhang et al. [40] has reported on using AlN/AlGaN superlattices for alleviating the crack problem of thick AlGaN films over sapphire substrates, and Wang et al.[56] noted that detailed x-ray measurements indicated that these superlattices were efficient in enhancing AlGaN mosaic block dimensions. Later, a modified PALE approach known as the migration-enhanced metalorganic chemical vapor deposition (MEMOCVD) technique was employed to further enlarge the AlGaN mosaic block dimensions [57]. In the MEMOCVD method, the duration of the group III and group V precursor pulses is further optimized in a pattern that allows beneficial surface migration of the reacting species on the growing film. This allows changing the V/III ratio from vanishingly small to several thousands, which greatly increases the probability that the Al- and Ga-adatoms migrate to their appropriate sites in the lattice. Very high-quality AlN and AlN/AlGaN superlattices were grown by this method. AlGaN device structures grown over these MEMOCVD AlN and AlN/AlGaN superlattices were also measured to be of superior quality, in terms of structural quality and minority carrier lifetime [58]. Figure 3 (a) presents the SEM image of a cracked AlGaN layer grown on a sapphire substrate with an AlN buffer layer and Fig.3(b) shows a cross-sectional transmission electron microscopic (TEM) image of a PALE-grown AlN on sapphire with the $Al_xGa_{1-x}N/Al_yGa_{1-y}N$ strain-relief superlattice that enables the growth of thick n-type AlGaN. Figure 3(c) and (d) show the experimental and simulated (0002) XRD 2θ-ω spectra for $AlN/Al_{0.85}Ga_{0.15}N$ superlattice layers, respectively. Figure 3(e) presents an atomic force microscopy image of a PALE grown AlN layer on a sapphire substrate with an $Al_xGa_{1-x}N/Al_yGa1-_yN$ strain-relief superlattice. Development of the AlGaN/AlN superlattice buffer layers enabled growth of highly doped n-AlGaN to a thickness of greater than 2.0 μm, enabling the development of UV-B and UV-C devices with submilliwatt- and later milliwatt-level output powers [59,60].

There are also several other approaches that have been explored to improve AlGaN quality. Kamiyama et al. used grooved GaN templates for AlGaN growth with the aim of bending the threading dislocations away from the growth direction [61]. A similar way which uses GaN templates and air-bridged lateral growth of AlGaN has also been demonstrated [62]. One limitation to those approaches is that they are only efficient in low Al-content AlGaN growth. These methods encounter difficulties in high-Al-content materials because of the very small lateral growth rate. Pioneering work on epitaxial growth and characterization of AlN and AlGaN layers over bulk AlN substrates was reported by several groups [63- 67]. Numerous advantages of bulk AlN substrates such as the possibility of homoepitaxial growth, potential transparency in the UV region, and high thermal conductivity, have been addressed. Widespread commercial availability of these bulk substrates of uniform quality can be expected to provide the ultimate solution for growth of crack-free high quality AlGaN films.

More recently, high temperature growth by the MOCVD method has been employed successfully to grow AlN layers with better structural quality. By the conventional MOCVD growth, the maximum growth temperature employed is around 1200°C. In the high temperature methods, temperatures in the range 1200-1600°C are used. The high temperature condition is expected to promote two-dimensional growth in the case of III-nitride semiconductors, especially AlN, as it causes increase of the diffusion length of cation species [68]. Balakrishnan et al. have investigated the AlN growth on SiC under high temperature conditions up to 1500°C and reported that their resultant layers contained a dislocation density as low as 10^6 cm^{-2} [69]. Similarly, the high temperature growth technique has been successfully employed to grow AlN and AlGaN layers on other substrates as well, and in many cases crack-free layers with high structural quality of thickness more than 6μm have been reported [70,71,72,73,74,75].

Figure 3. (a)
an Al
ima
stra
(c)
$Al_{0.8}$
on a

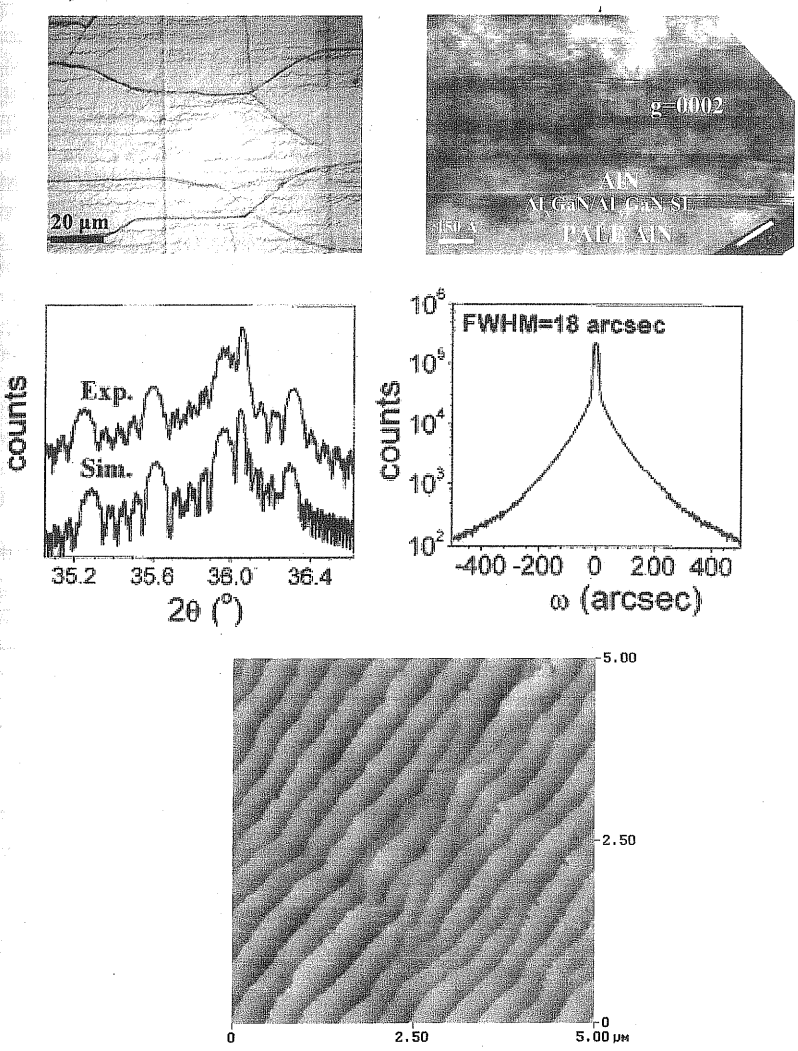

Figure 3. (a) SEM image of a cracked AlGaN layer grown on a sapphire substrate with an AlN buffer layer; (b) cross-sectional transmission electron microscopic (TEM) image of a PALE-grown AlN on sapphire with the $Al_xGa_{1-x}N/Al_yGa1-_yN$ strain-relief superlattice that enables the growth of thick n-type AlGaN; (c) Experimental and (d) simulated (0002) XRD 2θ-ω spectra for AlN/ $Al_{0.85}Ga_{0.15}N$ superlattice layers. (e) AFM image of PALE grown AlN layer on a sapphire substrate with $Al_xGa_{1-x}N/Al_yGa1-_yN$ strain-relief superlattice.

Another novel approach used recently to grow AlN films is to combine MOCVD and HVPE in a single growth chamber. This has been found to be effective to deposit 20 μm thick, crack-free single crystal AlN films over grooved basal plane sapphire substrates with lateral growth rates in excess of 2 mm/h. This approach, where MOCVD and HVPE growths can be carried out in the same reactor either sequentially or simultaneously in any arbitrary order, is referred to as metalorganic hydride vapor phase epitaxy (MOHVPE). The combination of MOCVD and HVPE in the same reactor affords the flexibility to grow buffer and device layers at growth rates ranging from 0.1–10 mm/h without removing the substrate. It is therefore ideal for the deposition of thick AlN buffers and deep UV light emission devices over substrates such as sapphire with excellent optical properties but a low thermal conductivity. In addition, the viability of the MOHVPE process for fast lateral epitaxy of AlN and a subsequent growth of high-quality UVC LED epilayers was demonstrated for the first time.

Energy gap bowing of $Al_xGa_{1-x}N$. In the design of UV light emitting devices, it is important to know the fundamental band gap of AlGaN over a large range of Al mole fractions. The results of absorption measurements performed at atmospheric pressure yielded the variation of the band-gap energy which was found to be $E_g(x) = 3.43 + 1.44\ x + 1.33\ x^2$ eV for the $Al_xGa_{1-x}N$ system [76]. There is a large nonlinear variation with concentration for the fundamental band gap. When the experimental bowing parameter of 1.0 is used, the relationship obtained is $E_g(x) = 6.2\ x + 3.43\ (1-x) - x\ (1-x)$, and this has been generally adopted [77].

Doping of $Al_xGa_{1-x}N$ materials.

n-type doping. The doping of AlGaN materials is still not established to the extent of the doping in GaN and InGaN. There is a rapid decrease in the conductivity for both doping types with increasing Al compositions. As the aluminium composition is increased, the band gap of the $Al_xGa_{1-x}N$ semiconductor increases and the ionization energies for silicon (most commonly used n-type dopant) and magnesium (most commonly used p-type dopant) increase, resulting in a lower ionization efficiency. In addition, the material quality is degraded with the increase of dopants and this causes poor mobility of carriers in the lattice. $Al_xGa_{1-x}N$ materials with low resistivity are specifically desired because most deep-UV light emitters are prepared on transparent sapphire, with a few initial demonstrations using bulk and pseudo-bulk AlN substrates. Both sapphire and AlN are electrically insulating and thus necessitate the fabrication of laterally conducting light emitting devices with both contacts on the same side of the wafer. Higher resistivity of the n-contact AlGaN layer results in non-uniform current injection in the light emitting device active area, known as current crowding. Current crowding leads to increased injection currents along the perimeter of the LED mesa [78].

As mentioned above, the MEMOCVD growth method has been shown to produce high-quality AlN and AlN/AlGaN superlattices for defect reduction in AlGaN and such defect reduction can greatly improve the doping efficiency by reducing compensating and scattering centers. As a result, room-temperature electron Hall mobilities exceeding 85 $cm^2/V{\cdot}s$ for n-AlGaN with Al molar fraction of 50 % have been obtained [79]. Using molecular beam epitaxy (MBE) Si doping in high-Al-mole fraction AlGaN alloys has been achieved with very high n-type carrier concentrations $\sim 10^{20}$ cm^{-3}, but with poor mobility [80]. No significant degradation of materials properties was reported. Si δ-doping, where basically an atomic plane of Si atoms was introduced as the electron source, has been introduced for a 340 nm UV LED structure whereby improved performance with output powers of 150 μW at a dc driving current of 100 mA has been achieved [81].

p-type doping. P-type doping of high Al-content AlGaN is even more challenging as the room temperature activation energy for the most commonly used acceptor Mg in p-type GaN is already a relatively high 250 meV. It increases for AlGaN such that it is difficult to achieve conduction in p-type AlGaN with aluminum composition greater than ~15-20%. In addition to increasing the device resistance, which results in Joule heating, it is very difficult to make an ohmic contact to p-AlGaN

films. Therefore, most researchers deposit a p-GaN film to the top surface to serve as a contact layer, with this film absorbing some of the UV emission. Even if one can inject holes effectively from the metal into the p-GaN material, such holes are then faced with a potential barrier before they can be transported across subsequent AlGaN barrier layers down to the quantum well. Holes that are trapped at the first interface set up an electric field which can attract electrons to bypass the quantum wells and hence recombine non-radiatively in the p-GaN layer, having a major impact on quantum efficiency. Several approaches have been suggested to enhance the Mg-doped AlGaN p-type conductivity. One method is to use either a short period or a large period superlattice (SPSL or LPSL) composed of Mg-doped AlGaN/GaN layers to replace conventional p-AlGaN [82- 85]. For the SPSL the period is very small, typically below 4 nm, hence minibands are formed, and vertical conduction of the p-SPSL should not be degraded. In the large period case, the period is typically larger than 15 nm, but the valence band discontinuity as well as the polarization fields can enhance the ionization of the acceptors in the AlGaN barriers and transfer holes into GaN wells. However, since the period is large, wave function coupling between neighboring wells is forbidden, which greatly reduces the vertical conductivity. As a result, this LPSL approach can only get good horizontal p-conductivity. Several groups have used Mg-doped AlGaN/GaN SPSL in 340-350 nm UV LED growth [86- 88].

The second approach was proposed by Shur et al., namely, using a p-GaN/p-AlGaN single heterostructure to achieve hole-accumulation at the interface [89,90]. The mechanism of this approach is similar to the LPSL approach. However, since in the p-GaN/p-AlGaN single heterostructure only one barrier exists for hole transport, the vertical conductivity can be greatly enhanced due to the high-density hole accumulation at the interface and the field assisted tunneling as well as thermionic emission. Most of the reported deep UV LEDs used this approach for hole injection into the active layers and get reasonably good powers [91- 97].

The third approach, δ-doping, has been investigated by Nakarmi et al.[98]. It was demonstrated that Mg δ-doping improves not only p-type conduction, but also the overall quality of p-type GaN and AlGaN. It was observed that the Mg δ-doping enhances the hole concentration while inducing no changes in the hole mobility.

DUV LEDs

Khan et al. reported the first UV-B LED with emission wavelength at 305 nm [39]. As before, the quaternary AlInGaN MQW active region was grown by PALE. Limitations in material quality, doping problems and insufficient thickness of the bottom n-AlGaN layers put severe limits on performance due to the high sheet resistance of the n-AlGaN, which immediately created a problem of poor current spreading in mesa geometry devices on sapphire. To overcome the current spreading problem a stripe geometry configuration was suggested.

The growth of thick (up to 2.5 μm) highly doped n-AlGaN was enabled after the development of novel AlGaN/AlN SL buffer layers [40] which resulted in a rapid development of improved UV-B LED devices. The submilliwatt operation for an LED with emission at 315 nm and the milliwatt operation for an LED with emission at 325 nm were next reported by Chitnis et al.[99,100]. This improvement was achieved by implementing the innovative SL buffer layer approach for growth of low sheet resistance n-AlGaN, by optimizing the device geometry for better current spreading, and by introducing flip-chip packaging for improvements in thermal management and light extraction. The problem of lateral current crowding with sapphire- based deep UV LEDs has been analyzed and the optimization of the device geometry through the use of an interdigitated multi-finger geometry was suggested by Shatalov et al.[101,102]. Optimization of the growth approaches and optimization of the LED structural design along with advanced packaging techniques resulted in milliwatt dc operation of LEDs with the emission at 325 nm as reported by Chitnis et al. [93,103,104]. The initial submilliwatt operation of a nitride-based LED emitting in the UV-C band was demonstrated in 2002 by Adivarahan et al., a device which operated at 285 nm

with a cw output power of 10 μW at 60 mA drive current [41,105]. This device yielded 0.15 mW with 400 mA applied under pulsed conditions. With advancement of contact processing technology, they were able to achieve output powers as high as 0.25 mW at 650 mA under pulsed pumping conditions with the next generation of devices. The output power was shown to be thermally quenched by at least 10 times as the operating temperature was raised from 100 K to room temperature under pulsed conditions.[106] These data indicated that non-radiative recombination at defects rather than a lack of hole transport to the quantum well is the key contribution to the low quantum efficiency of 285 nm devices. Further optimization of the AlN buffer layer quality by means of PALE has been reported by Zhang et al.[57,79] which enabled improvements in the material quality of the lower n-AlGaN bottom cladding layer as well as the MQW layers, and these advances resulted in a rapid increase of the LED output power up to milliwatt levels [91]. By optimization of the quality of the AlGaN layers grown over sapphire substrates, several groups have now reported improved LED devices with emission around 280 nm [107-110]. While the majority of the reports described the optimization of AlGaN growth by MOCVD, others have presented the use of molecular beam epitaxy (MBE) with an ammonia source as an alternative approach, along with innovative short-period SL cladding layers [111-114].

Despite the advancements made in this field, the quantum efficiency of these UV-C LEDs remained much below 1 % and worse yet, the emission spectrum consisted of several peaks: a near band-edge emission from the quantum well and longer wavelength peaks associated with deep-level transitions in barrier layers [92,115]. This stimulated a second round of device structure and growth optimizations, and many groups reported a significant improvement of device output power and spectral purity [94,97,116-118]. Fisher et al.[97] reported dc power levels as high as 1.34 mW at 300 mA for large area 290 nm devices, while achieving external quantum efficiency as high as 0.18 % for devices with smaller areas. Later, Sun et al.[59] and Zhang et al.[60] demonstrated high power UV-C LEDs with emission around 280 nm with dc output power around 1 mW at 20 mA and corresponding external quantum efficiency of ~ 1.1 %.

UV-C LEDs with emission wavelength in the range 265 nm – 270 nm have also been reported by several groups. Remarkable device performance was achieved by Yasan et al. [96] who reported submilliwatt dc and as high as 4.5 mW pulsed output powers at 267 nm corresponding to a quantum efficiency of ~ 0.1 %. These power levels have been further increased by Adivarahan et al.[95] and Bilenko et al.[119], who reported quantum efficiencies of 0.4 % and 0.2 % at 269 nm and 265 nm, respectively. Submilliwatt pulsed operation of deep UV-C LEDs with emission wavelength as short as 250 nm were reported in 2004 by Adivarahan et al.[120]. Subsequently, Allerman et al.[117] obtained an electroluminescence peak from a UV-C LED structure at the wavelength as short as 237 nm, demonstrating the possibility for further reduction of the emission wavelength towards 200 nm.

The dc operation of LEDs with wavelength shorter than 260 nm becomes severely limited by the lack of conductivity of the bottom Si-doped AlGaN cladding layer since the Al molar fraction required for transparency increases above 70%. To improve the current spreading in LEDs with high Al molar fractions in the AlGaN cladding layers, an interconnected micro-pixel design has been adapted.[121,122]. This use of micro-pixels was first introduced for III-nitrides by Mair et al.[123] to improve the light extraction from a AlGaN/GaN slab via the formation of microcavities, and the approach was then used in blue [124] and UV-A LEDs.[81] The micro-pixel LEDs design was further extended to the formation of photonic crystals [125] by the reduction of the size and the period of the array elements [126,127]. An LED design with interconnected micropixels separated by the n-AlGaN contact metal was also shown to be very efficient in achieving the desired uniform current pumping for deep UV-C LEDs, and devices with emission at 255 nm with 1 mW dc and 3.4 mW pulse powers and corresponding maximum quantum efficiencies of 0.14 % and 0.3 % (in dc and pulse pumping, respectively) were recently demonstrated by Khan et al.[128] Normalized electroluminescence spectra of deep UV LEDs are shown in Fig.4. All devices exhibit a strong peak corresponding to near band- edge emission from the MQW active region with full width at the

Figure 4. Ele

half maximu
composition
intensity of
360 nm –
characteristi
(and quantu
lower dopin
Increasing o
devices. Thu
effective so
reported 24
voltages we
packaged de

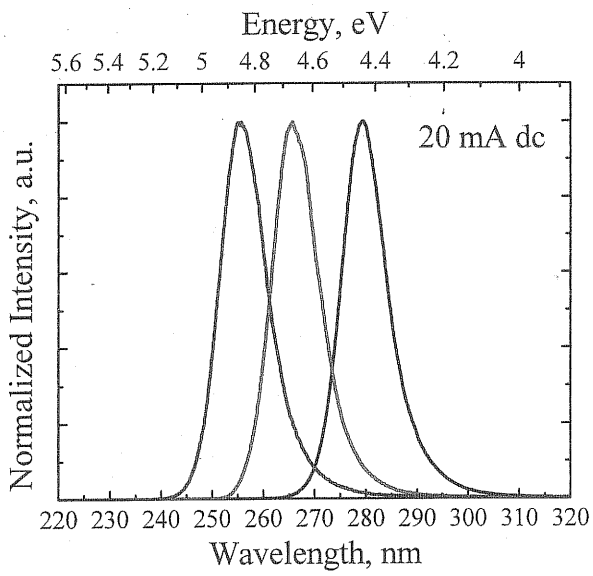

Figure 4. Electroluminescence spectra of deep UV LEDs under 20 mA dc pump current.

half maximum of about 10 nm. Hence, by proper choice of the AlGaN MQW active region composition the emission wavelength can be effectively tuned from 255 nm to 280 nm. The intensity of the main emission peak is stronger than that of long wavelength emission peaks (at 360 nm – 500 nm) by at least 300 times (not shown). Output powers vs. pump current characteristics for these deep UV LEDs are plotted in Fig.5. As can be seen in the Fig.5 the power (and quantum efficiency) strongly reduces with emission wavelength. This is a consequence of lower doping efficiency and reduced material quality of AlGaN layers with very high Al content. Increasing operation voltage also leads to early power saturation in dc pumping for square geometry devices. Thus, as described above, interconnected micro-pixel array geometry was shown to be an effective solution for devices with shorter emission (i.e. 255 nm). Recently, Deng et al.[129] reported 247 nm deep-UV LED by employing an MEMOCVD grown structure. The turn-on voltages were lower than 8V at 20 mA current. Power levels of 0.3 mW were achieved for the packaged devices driven at 90 mA DC current.

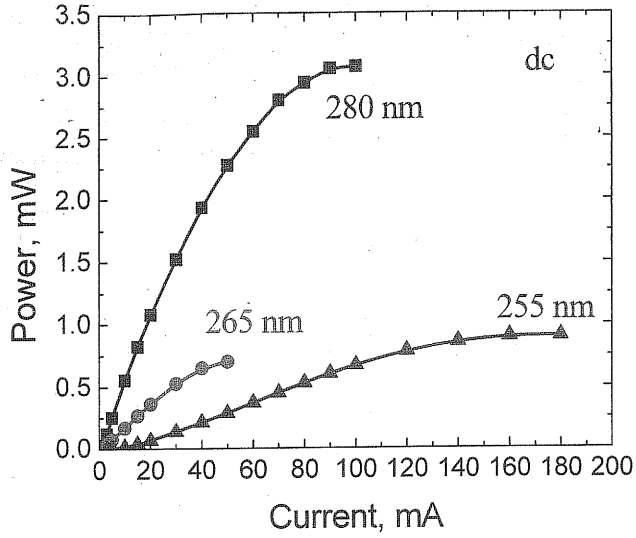

Figure 5. Output power vs. dc pump current characteristics of packaged deep UV LEDs. Data for 100 μm x 100 μm square device for 280 nm (black) and 265 nm (red) emission LEDs and 10x10 micro-pixel array LED for 255 nm (blue) emission LED are shown.

Recent efforts on the fabrication of DUV LEDs on PLOG grown thick (> 15 μm) low-defect AlN buffer layers and by the MOHVPE technique have yielded devices with significant improvement in performance. The excellent thermal conductivity of AlN enabled the devices from getting pre-matured power saturation. The lower-defects and the thick AlN templates resulted in a much superior thermal management which translated to 280 nm LED's lifetimes increasing to well above 2000 hours. Figure 6 presents a typical power density vs current density, measured under dc bias, for a 285-nm LED fabricated by the MOHPE method. It is very significant that small periphery MOHVPE LEDs, such as a 50μm diameter device, are able to sustain extremely high current densities, up to 4000 A/cm^2, without the power saturating. This is an indication of the improved thermal dissipation for the LEDs grown on the MOHVPE AlN templates compared to the conventional MOCVD grown devices. The arrow on Figure 6 shows the current density for power saturation for a flip-chipped and fully packaged conventional first generation MOCVD grown UV LED on a sapphire substrate. The conventional LED output power saturated at approximately 0.5 kA/cm^2 (delivering an output power density of 3 – 5 W/cm^2) under cw bias condition. It should be noted that for conventional UV LEDs, the saturated input current density is increased by about 80% when the devices were flip-chipped to a heat sink and placed on a TO header. The MOHVPE LEDs are expected to handle current densities well in excess of 4.0 kA/cm^2 after packaging.

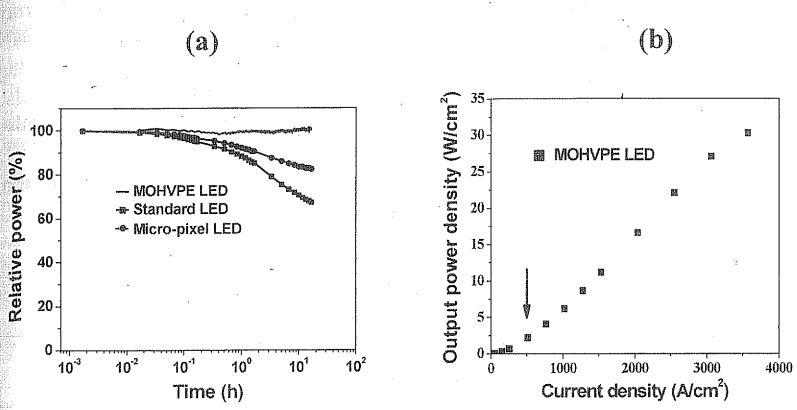

Figure 6 (a). Lifetime reliability of MOHVPE 280nm LED in comparison with a standard LED and a micro-pixel LED; (b) Comparative cw output power density plot of a standard deep-UV LED and the LED formed by MOHPE AlN.

Taniyasu et al. have reported the successful control of both n-type and p-type doping in AlN and this allowed them to develop an AlN PIN (p-type/intrinsic/n-type) homojunction LED with an emission wavelength of 210 nm, which is the shortest reported to date for any kind of LED [130]. Their LED structure was fabricated on a SiC substrate.

Critical issues related with DUV LEDs. Most DUV LEDs are prepared on transparent sapphire substrates, which are totally insulating. The current applied to the DUV LED must be spread laterally through an n-type AlGaN layer near the substrate, and a high resistivity in such a film limits the extent of current spreading, leading to crowding along the perimeter [131]. Passage of the current through high resistance films generates heat. There are even worse problems with p-type AlGaN. Since it is very difficult to make an ohmic contact to p-AlGaN films, most researchers apply a simple p-GaN film to the top surface to serve as a contact layer, and this film can absorb UV emission. Even if one can inject holes effectively from the metal into the p-GaN material, such holes are then faced with a potential barrier before they can be transported across subsequent AlGaN barrier layers down to the quantum well. Holes that are trapped at the first interface set up an electric field which can attract electrons to bypass the quantum wells and hence recombine non-radiatively in the p-GaN layer, which has a major impact on quantum efficiency. Hence in terms of device performance these issues create major challenges: uniformity of current spreading, carrier injection, light extraction and thermal management and these issues are discussed in separate sections later.

Uniformity of lateral current spreading. In the case deep UV LEDs formed on the electrically insulating sapphire substrates, achieving uniform lateral current spreading is a major issue. This problem has been analyzed and an interdigitated multi-finger geometry was demonstrated by Chitnis et al. Using this electrode geometry, the lateral distance between adjacent n-contact metallization is reduced, leading to more spatially uniform current injection throughout the active region of the device. This allows for larger active areas than those permitted by square or circular geometry LEDs. To improve the current spreading in LEDs with high Al molar fractions in the AlGaN cladding layers, an interconnected micro-pixel design has also been adapted [53,132]. The use of micro-pixels was first introduced for III-nitrides by Mair et al.[133] to improve the light extraction from a AlGaN/GaN slab via the formation of microcavities, and the approach was then